An Analysis of L1-C/A Cross Correlation & Acquisition Effort in Weak Signal Environments

Sana Ullah Qaisar
School of Surveying & Spatial Information Systems
University of New South Wales, Sydney 2052, Australia
Tel: +61 (2) 93854208 Fax: +61 (2) 93137493
s.qaisar@student.unsw.edu.au

Andrew G Dempster
School of Surveying & Spatial Information Systems
University of New South Wales, Sydney 2052, Australia
Tel: +61 (2) 93856890 Fax: +61 (2) 93137493
a.dempster@unsw.edu.au

ABSTRACT

Modern mobile devices are now equipped with GPS-receivers to provide E911 and other location based services. Working indoors, the GPS receiver is likely to experience a situation where some of the received signals are stronger than others. These strong signals can prevent the acquisition of a desired weak signal or lead to false acquisition, due to high cross correlation between the strong and weak signals. The C/A Gold code used in GPS L1 signal has an inherent correlation protection of about 24 dB. This becomes inadequate for weak signal acquisition in the presence of multiple strong signals. Various cross correlation mitigation techniques are used to deal with this problem. The impact of cross correlation on weak signal acquisition largely depends on the relative power level and carrier offset of the desired weak signal with reference to the strong interfering signals. This paper first presents an analysis of the L1-C/A cross correlation in the presence of multiple strong signals under different conditions of relative Doppler offset and dwell time. Acquisition of weak signals with different SNR levels is then performed under these conditions, using the "Tong" search algorithm and the results of acquisition are presented. The results indicate that, for certain relative Doppler offsets, extended dwell times assist in combating the cross correlation noise hence improving the detection probability.

KEYWORDS: cross correlation, acquisition, probability, interferer, dwell time, relative Doppler offset.

1. INTRODUCTION

A GPS receiver operating in weak signal environments (like inside buildings or urban canyons) can simultaneously receive strong LOS (line-of-sight) signals as well as attenuated weak signals from satellites. Similar situations may also occur when a GPS receiver is operating in the proximity of a pseudolite. Cross correlation between the local replica of the desired weak signal and a strong signal can exceed the detection threshold, leading to false

acquisition, under such conditions (Glennon *et al*, 2005). It becomes worse as the number of strong signals (which here can be considered to be interferers) increases. The inherent correlation protection of the C/A Gold codes is about 24 dB (Morton *et al*, 2003). This becomes inadequate where acquisition of weak signals, coexisting with strong interferers, is desired. A signal is considered "weak" if its power level is approximately 24 dB (cross correlation margin) less than the reference strong signal. Weak GPS signal are typically acquired by using a combination of the coherent and non-coherent integrations for accumulating the signal energy. This however does not directly address the cross correlation problem (Shanmugam, 2006).

In the first part, this paper examines details of the L1-C/A cross correlation performance, in the presence of multiple strong signals with different relative Doppler offsets and dwell times conditions. Cumulative probabilities of cross correlation results are used for assessing the correlation performance of the L1-C/A signal under these conditions. In order to use realistic Doppler offsets between pairs of satellites, GPS satellites were observed over Sydney and the probability distribution of Doppler offset is generated. In the second part of the paper, acquisition of weak signals, coexisting with strong interferers is performed, using the "Tong" search algorithm (Tong, 1973). Different Doppler offsets and dwell times (integration intervals) are trialled to observe the corresponding cross correlation effects. The results of acquisition indicate that for certain relative Doppler offsets, longer integration intervals assist in combating the cross correlation noise, hence improving the detection probability.

2. CROSS CORRELATION ANALYSIS

The cross correlation performance of the L1-C/A signal is analysed in this section. Separate subsections provide relevant details on the significance of various parameters in the cross correlation performance of the L1-C/A signal.

2.1 Raw Full Length C/A Code

For this case, 1 epoch of raw C/A code (1023 chips) is used. We describe the code as "raw" as it needs not be considered as a signal but simply a sequence of 1s and -1s. It could also be thought of as, a code with one sample per chip. Figure 1 illustrates the cumulative probability of cross correlation for this case. The figure is generated from the result of cross correlation (1023 values) between PRN-18 and PRN-1. The vertical axis in the figure gives the probability of a certain range of cross correlation values along the horizontal axis. And the horizontal axis represents the cross correlation power with reference to the autocorrelation peak, in dB. The autocorrelation peak of a signal like this is 1023. Of the 1023 values in the cross-correlation result, 735 (71.85 %) have the value -1, i.e. 60 dB down from 1023, 136 (13.29%) have the value -65 and 152 (14.86%) have the value 63, totalling 28.15 % that sit at around 24dB down from the autocorrelation peak. This means that the C/A Gold code has correlation protection of about 24 dB. Nearly identical plots are obtained for cross correlating any other two PRN codes (Dempster, 2006).

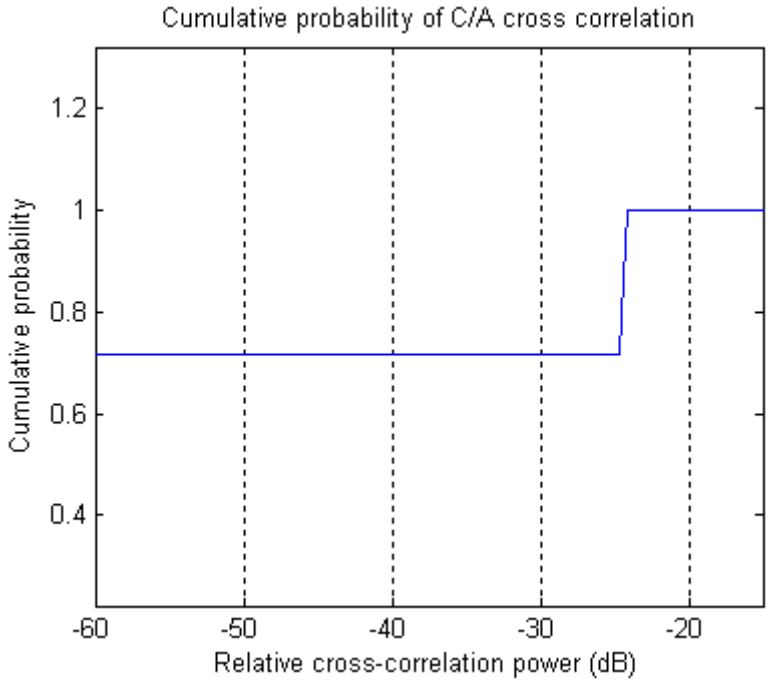

Figure 1. Cumulative probability of raw C/A code cross correlation

2.2 Synchronously Sampled C/A Code

In this case, the 1023 chips in the C/A code period are sampled in such a way that there is exactly the same number of samples in each chip. Figure 2 shows the cumulative probability of cross correlation between two (PRN-18 & PRN-1) synchronously sampled C/A codes. The result indicates that the sampling does not gain any improvements in the correlation protection. The same behaviour is observed for various sampling rates. The only difference, when compared to the raw case is that the curve becomes "smoother" as the sampling rate is increased. This is because individual cross-correlation results here are interpolating between the values in the raw case. Figure 3 illustrates the (asynchronously sampled) case where the sampling rate is not a multiple of the chip rate, e.g. the 5.714 MHz used in the Zarlink GP2015 RF front end (Zarlink Semiconductor, 2005). This causes smoother curves to be observed when compared to a synchronously sampled C/A code case for similar sampling rates.

2.3 L1-C/A Signal

In this case, the L1-C/A signal is considered where C/A code modulates the L1 carrier. The cross correlation between two L1 carriers modulated by different PRN codes (18 & 1) is performed. The signals use a sampling frequency of 5.714 MHz. and intermediate frequency of 1.405 MHz, consistent with the Zarlink GP2015 RF front end (Zarlink Semiconductors, 2005).

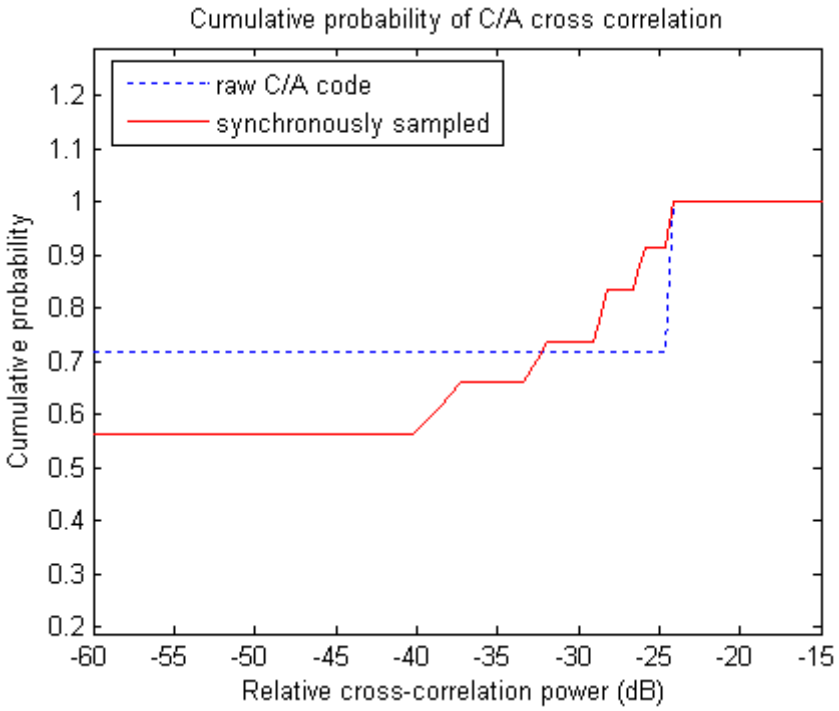

Figure 2. Cumulative probabilities of synchronously sampled C/A code cross correlation (5 samples per chip)

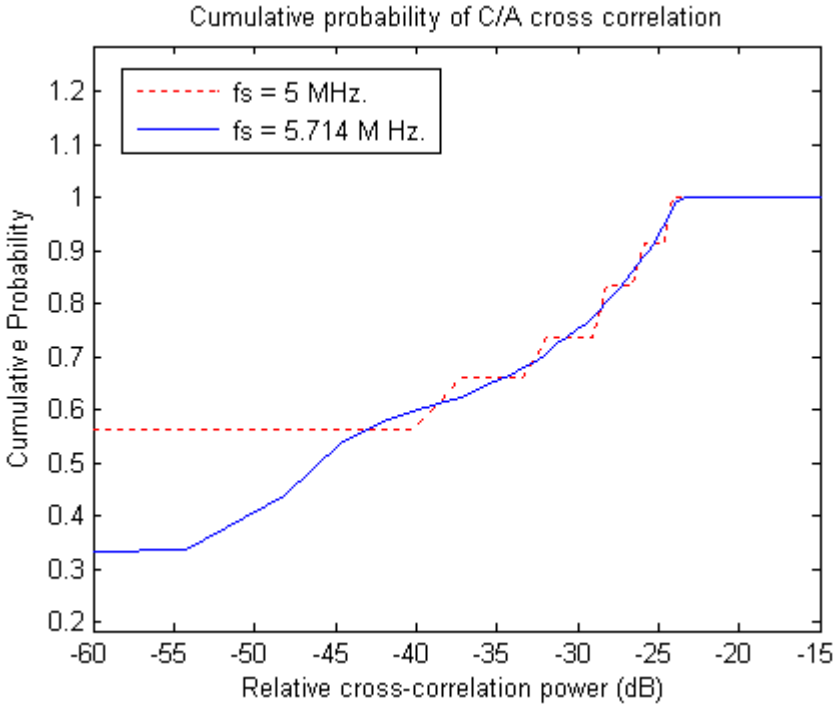

Figure 3. Cumulative probabilities of asynchronously sampled C/A code cross correlation sampling rate = 5.714 MHz. (used in the Zarlink GP2015 front end chip)

Cumulative probabilities of this case are shown in Figure 4, for relative Doppler offsets (carrier offset between the two signals being considered for the cross correlation) of zero and 1 kHz. The figure indicates that the cross correlation becomes worse for this case. This is because after mixing with the carrier (in the modulation process), Gold codes loose their

original property of low cross correlation (Spilker, 1996). The impact of relative Doppler offset on the cross correlation performance is discussed in the following section.

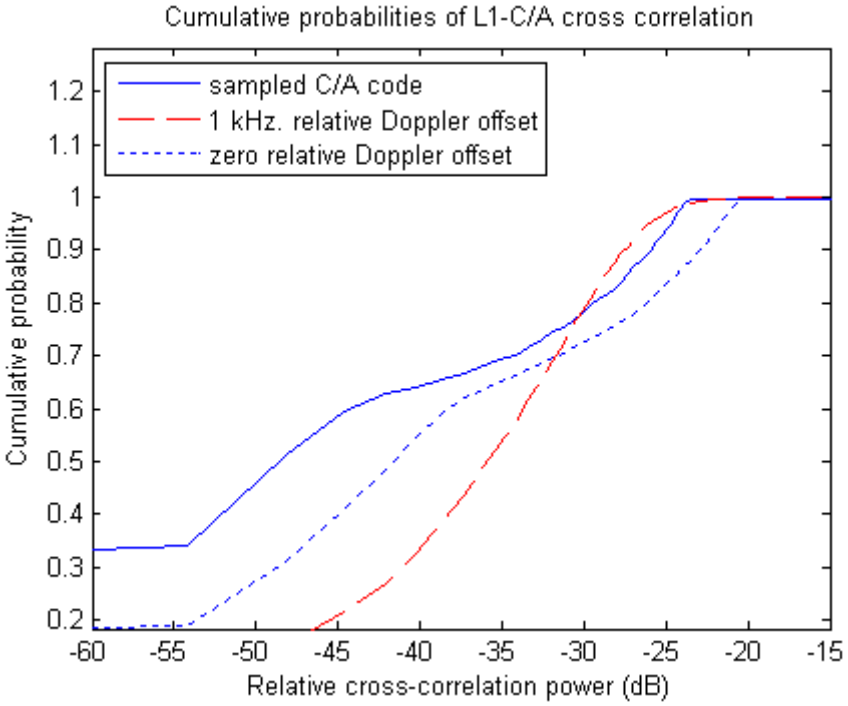

Figure 4. Cumulative probabilities of original and modulated C/A Gold codes cross correlation

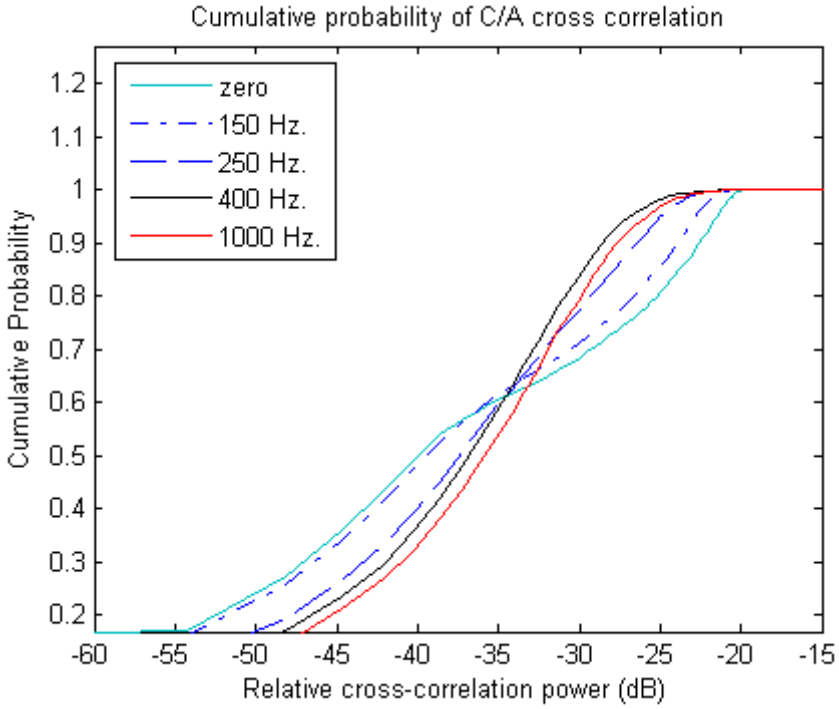

Figure 5. Cumulative probabilities of L1-C/A cross correlation with different relative Doppler offsets

2.4 The Doppler Offset

In this case, results of cross correlation between two satellites with different relative Doppler

offsets are observed. Figure 5 shows cumulative probabilities of these results. It can be observed that the correlation protection is worst for the 'zero' relative Doppler offset and it improves as the relative Doppler offset gets away from zero until at about 400 Hz. No further improvements in the cross correlation performance are observed, for the relative Doppler offsets beyond (about) 400 Hz. This limiting effect is shown in Figure 5 by the 1 kHz relative Doppler offset curve. Figure 6 shows cumulative probabilities of cross correlation between two signals with relative Doppler offset in the range of +/- 5 kHz. at steps of 500 Hz. A cluster of similar curves is observed for all relative Doppler offsets above 500 Hz.

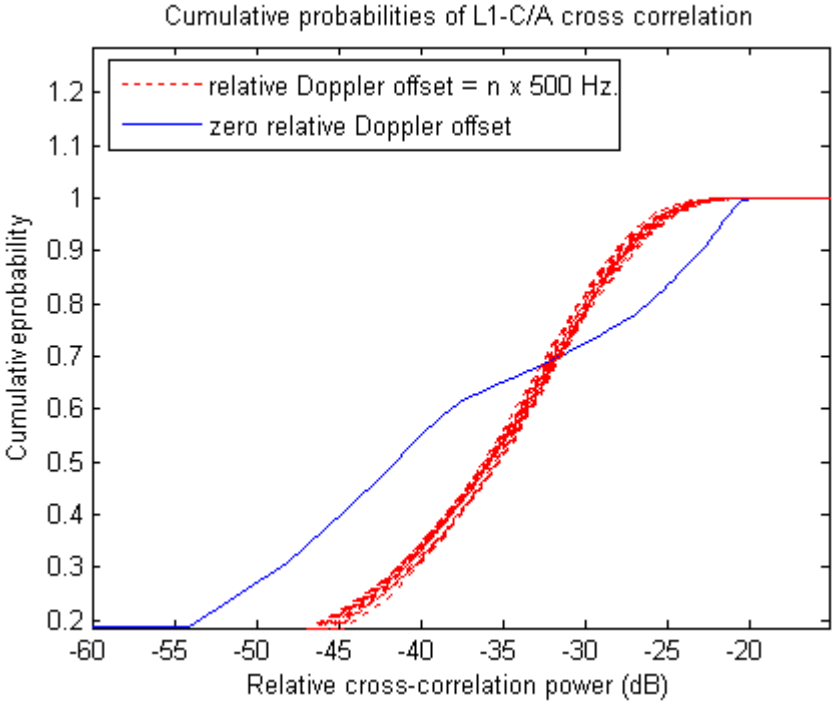

Figure 6. Cumulative probabilities of L1-C/A cross correlation with relative Doppler offsets of *n* $\times$ 500 Hz. (n = $\pm$1, $\pm$2, ……,$\pm$10)

2.5 The Dwell Time

For the raw C/A code, cumulative probability curves for integration periods of *m* milliseconds (*m* integer) are identical to that for 1 millisecond. However, performance of modulated satellite signals is improved for longer integrations because the relative Doppler offset phase is not correlated with the code. This is shown in Figure 7 for relative Doppler offsets of 200 Hz. and 500 Hz. For the zero relative Doppler offset, there is no improvement in the cross correlation performance with integration periods (IP's) longer than 1 millisecond (Glennon *et al*, 2006). Cumulative probabilities for the zero relative Doppler offset case are shown in Figure 8. When the relative Doppler offset is an integer multiples of 1 kHz, the code of strong signal is modulated by the corresponding relative Doppler offsets (multiples of 1 kHz.) and the signal energy accumulated over any 1 millisecond segment are exactly the same. This is because the phase of the relative Doppler offset is correlated with the C/A code repeating every 1 millisecond. (Morton *et al* in 2003). Hence again for this case, as shown in Figure 9, curves for integration periods of *m* millisecond (*m* integer) are identical to that for 1 millisecond. It is clear from all these figures
that for the relative Doppler offsets, (relatively) away from *d* kHz. (*d* = 0, $\pm$1, $\pm$2, …..), increased dwell times significantly reduce the effect of cross correlation.

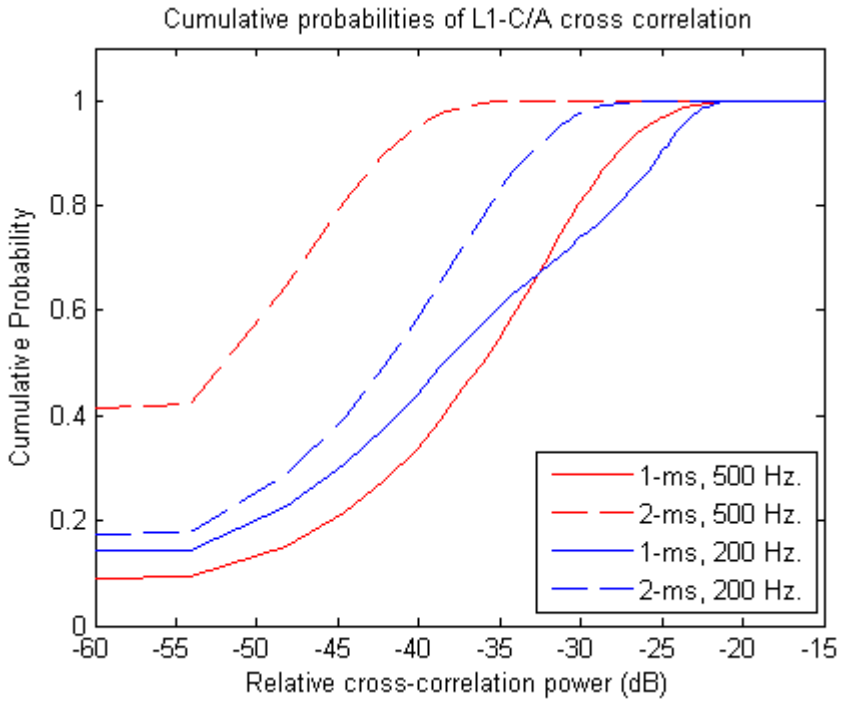

Figure 7. Cumulative probabilities of L1-C/A cross correlation with different IP's and relative Doppler offsets of 200Hz & 500 Hz.

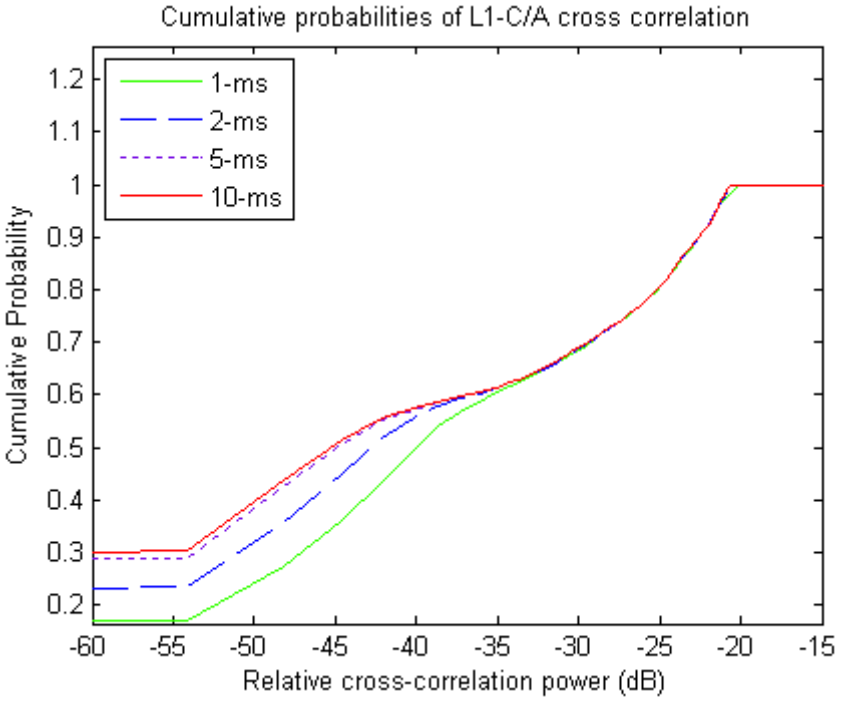

Figure 8. Cumulative probabilities of cross correlation with different IP's for zero relative Doppler offset

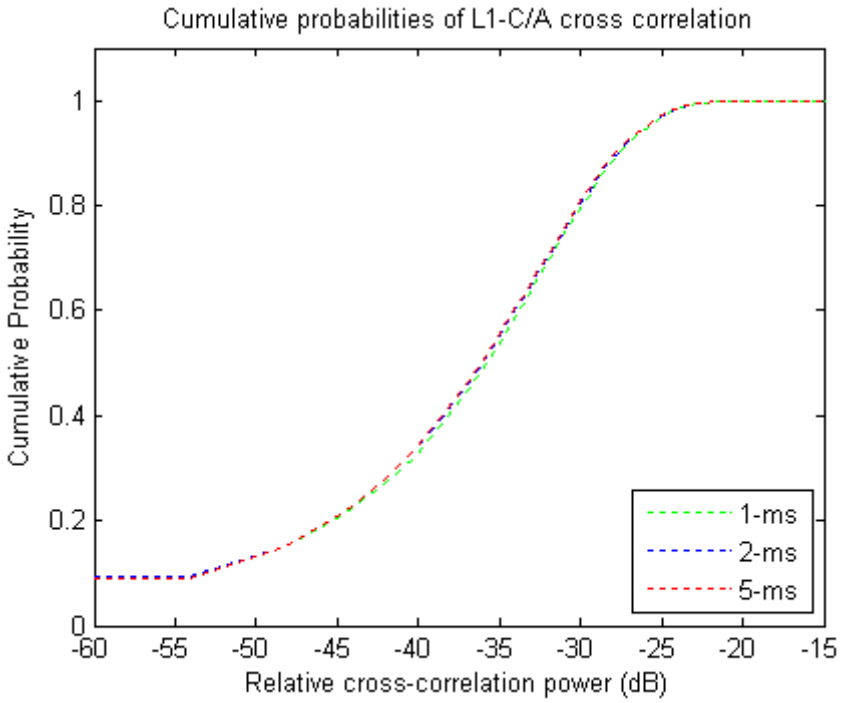

Figure 9. Cumulative probabilities of L1-C/A cross correlation with different IP's for a relative Doppler offset of 1 kHz.

2.6 The Doppler Offset Observations

In order to simulate real world scenarios, the carrier offset between the desired weak signal and strong interferers must be chosen carefully. For the purpose of this analysis, skies of Sydney were observed every 60 minutes over the course of 24 hours in real time. In each observation, the Doppler estimate of each of the visible satellite above 10 degrees elevation is recorded and the relative Doppler offset between each pair of satellites is computed. Table 1 shows a particular observation record.

Satellite PRN	24	30	12	5	6	7
24	0	1540	3920	2850	-680	-1160
30	-1540	0	2380	1310	-2220	-2700
12	-3920	-2380	0	-1070	-4600	-5080
5	-2850	-1310	1070	0	-3530	-4010
6	680	2220	4600	3530	0	-480
7	1160	2700	5080	4010	480	0

Table 1. A particular Doppler offset observation record

Figure 10 (generated from 24 observation records) gives the probability distribution of the relative Doppler offset between two satellites. The corresponding cumulative distribution is shown in Figure 11. Realistic Doppler distribution can now be generated by reading off the relative Doppler offsets at uniformly distributed points in the vertical axis in Figure 10. The Doppler offsets used for the experiments are then randomly chosen from this space.

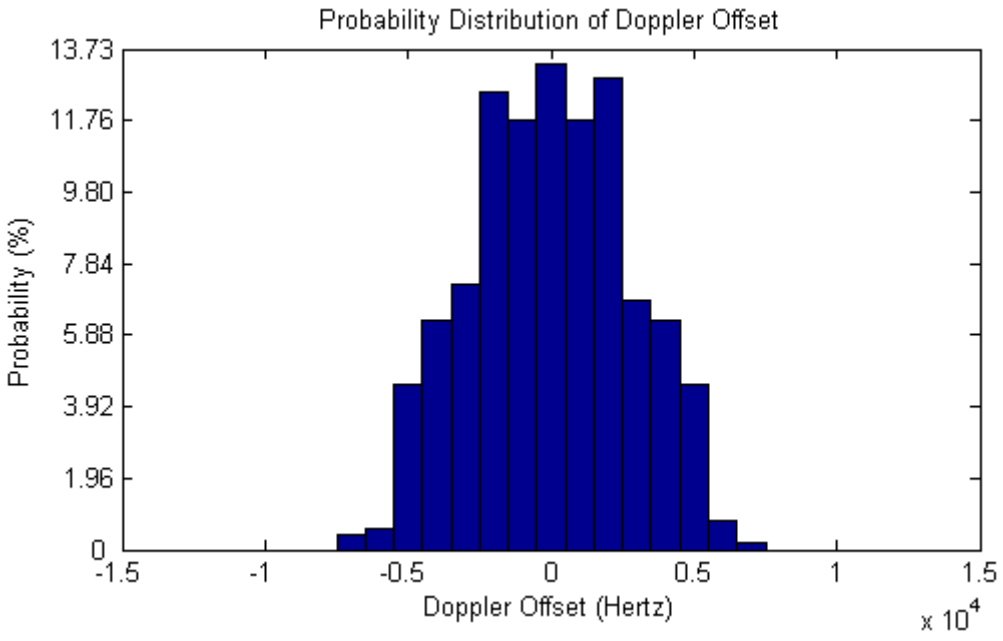

Figure 10. Probability distribution of relative Doppler offset between two satellites over Sydney

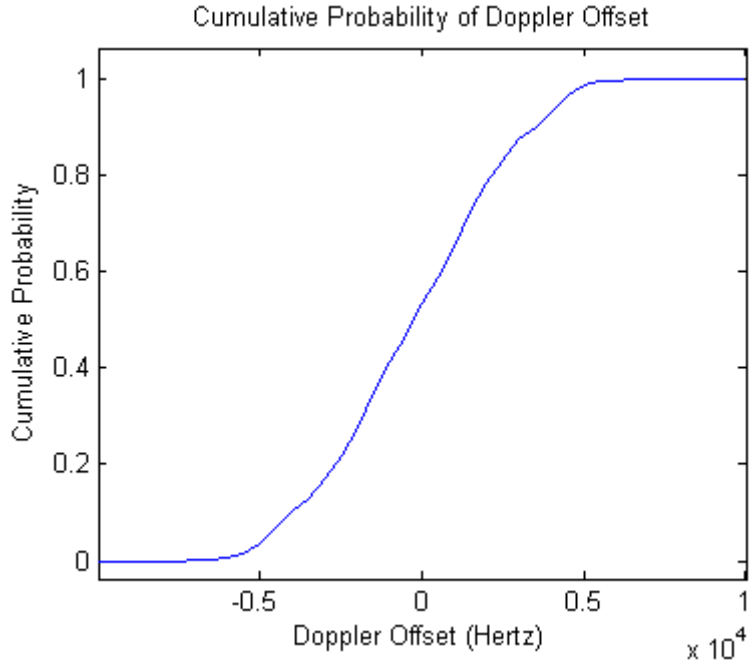

Figure 11. Cumulative distribution of relative Doppler offset between two satellites

2.7 Multiple Strong Signals

Figure 12 (zoomed in Figure 13) illustrates the cross correlation performance of L1-C/A signal in the presence of one, two, three and four strong signals respectively. To generate each of the cumulative probability curves in Figure 12, pairs of satellites are randomly chosen from a large set of satellites. For each pair, the cross correlation is performed for a number of randomly chosen (from the curve in Figure 11) relative Doppler offsets. Cross correlation results of individual cases are then averaged to produce final values for generating each curve. It can be observed from Figure 12 and Figure 13 that the cross correlation protection of the

L1-C.A signal decreases as the number of strong interferers increases.

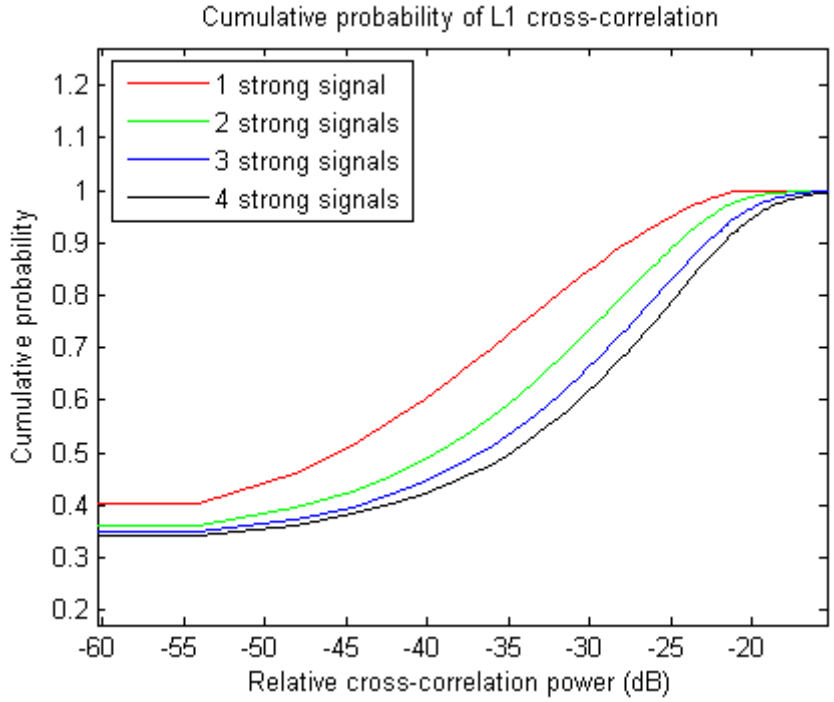

Figure 12. Cumulative probabilities of L1-C/A cross correlation in the presence of multiple strong signals

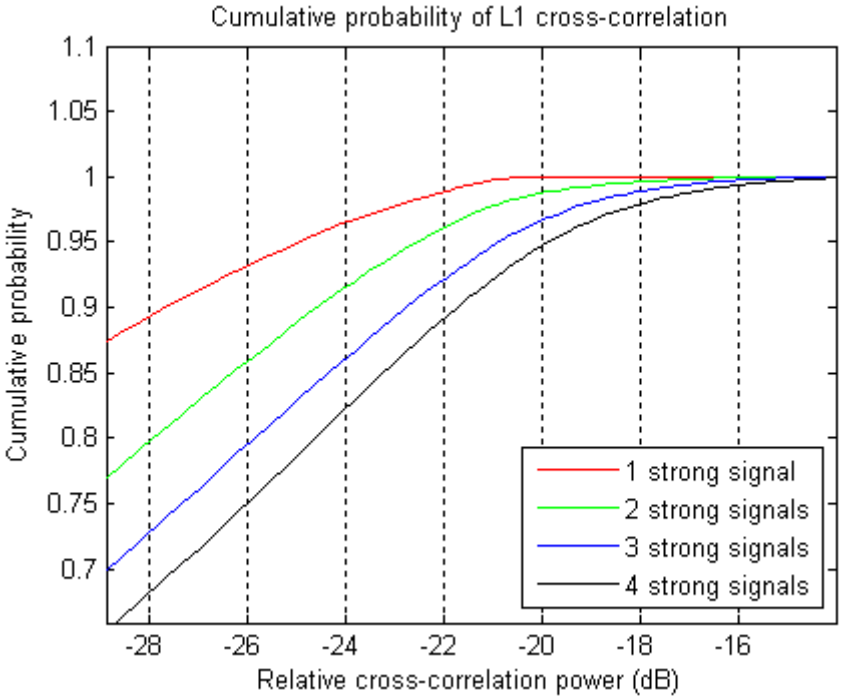

Figure 13. Cumulative probabilities of L1-C/A cross correlation (zoomed) in the presence of multiple strong signals

3. SIGNAL ACQUISTION

3.1 The Signal Search Algorithm

The "Tong" detector (Tong, 1973) is a sequential variable dwell time detector with a reasonable computation burden and proves good for acquiring signals with low SNR levels. It is a suboptimal search detector with an average factor of only 1.58 longer than the optimal maximum length sequence detector (Ward Phillip W. *et al*, 2006). The Tong detector sets relatively lower detection thresholds, V_t for a certain desired probability of false alarm $P_{fa.}$ In the Tong search algorithm, the integrated correlation envelope (approximated by) $\sqrt{I^2+Q^2}$ is computed every "T" (dwell time) interval and compared with the threshold V_t. During the signal search, in each cell (one code phase in a particular Doppler bin), the up/down counter K is incremented by one if the envelope exceeds the threshold, otherwise it is decremented by one. If the counter has reached maximum count value A, the signal is declared 'present' and the search is terminated. Similarly if the counter contents reach zero, the signal is declared 'absent' and the search is terminated. So that the Tong detector is not trapped into an extended dwell in the same cell, under certain poor signal conditions, another counter ($K_{\max}$) sets the limit on maximum number of dwells in a cell. Table 2 lists the search parameters used in this work.

K	A	P_{fa}	$K_{\max}$	fs (MHz.)	IF (MHz.)
2	10	10 %	11	5	1.405

Table 2. Settings for Tong search

In this work, the signal is searched in the 'correct' Doppler bin and is actually present at 200th sample (cell) code offset. The search is performed across 200 cells and the number of dwells (N) is recorded. The detection threshold V_t is set by equation (1)

$$V_t = \sigma\sqrt{-2\ln P_{fa}} \qquad (1)$$

Where σ^2 is the RMS noise power (Kaplan *et al*, 2006).To acquire very weak signal, usually blocks from coherent integration are combined incoherently for achieving the desired processing gain (Morton et al, 2003). In this analysis, extended dwell times up to 150 milliseconds are used without considering the navigation data modulation.

4. ACQUISTION RESULTS

4.1 Acquisition Results in the Absence of Strong Signals

A specific search space is provided to the Tong detector for different conditions of the SNR levels (of the desired weak signal), relative Doppler offsets (between the desired and interfering signals) and the dwell times. Table 3 gives the number of searches (N) performed to acquire the signal with given SNR (dB) and dwell time T (ms), in the absence of any strong signal. The threshold (V_t) is kept constant for each T. The numbers in Table 3, depict an estimate of number of searches required for signal acquisition under given conditions and may slightly vary with random thermal noise. A value of N around 450 states the signal as

'acquired' reliably.

SNR	T = 10 ms	T = 50 ms	T = 100 ms	T = 150 ms
-35 dB	452	460	460	460
-40 dB	-	450	457	436
-45 dB	-	-	437	429
-50 dB	-	-	432	433

Table 3. Number of acquisition searches in the absence of strong signals (- indicates not acquired)

Similar values of N can be observed all across the table. This is because very long dwell times are used and no false acquisitions are observed. It can also be observed from Table 3 that longer IP's assist in acquiring weaker signals.

4.2 Acquisition in the Presence of Multiple Strong Signals

Tables 4 (a, b, c, d) give the number of searches (N) performed to acquire the signal in the presence of multiple strong signals, under different dwell times T (ms) and relative Doppler offsets Δf (Hertz) conditions. The strong signals used for this analysis have SNR of -19 dB each as used by Morton *et al*, 2003. A value of N like "x/y" indicates that the search algorithm produced "x" false alarms in a total of "y" searches without acquiring the signal. It can be observed from these tables that for the zero relative Doppler offset, extended dwell times do not assist in preventing the cross correlation noise. For example in Table 4(a), the weak signal with SNR level of -45 dB could not be acquired with up to 150 miliseconds of integration period. On the other hand the same signal is successfully acquired with IP's of 100 and 150 milliseconds for the relative Doppler offsets of 250 Hz. and 500 Hz. At the same time it can be observed that the number of searches (N) and rate of false alarms significantly increase for the zero relative Doppler offset case. For example in Table 4(a), for T=100, -45 dB signal is successfully acquired in 442 searches (Δf = 250) without any false alarm while with the zero relative Doppler offset, it could not be acquired in 608 searches with 27 false alarms (608/27). It can be observed that these figures get worse as more strong signals are introduced into the analysis. These results of acquisition verify our analysis of the L1-C/A cross correlation in the presence of multiple strong signals, under different conditions of relative power levels and Doppler offset between the desired weak signal and strong interferers. Note that each value of N in the acquisition results is obtained from single trial, for the given conditions. The interpretation of these tables can be improved by considering average of several iterations for generating each value of N .

SNR	T = 10			T = 50			T = 100			T = 150		
	Δf	Δf	Δf	Δf	Δf	Δf	Δf	Δf	Δf	Δf	Δf	Δf
	0	250	500	0	250	500	0	250	500	0	250	500
-35	511	443	430	767/26	454	451	645/26	468	454	636/31	472	472
-40	-	425	430	642/24	429	446	606/24	460	460	642/26	452	448
-45	-	-	-	628/20	-	-	608/27	442	454	645/30	440	442
-50	-	-	-	600/16	-	-	639/25	-	-	665/28	446	431

(a). Single strong signal case

SNR	T = 10			T = 50			T = 100			T = 150		
	Δf	Δf	Δf	Δf	Δf	Δf	Δf	Δf	Δf	Δf	Δf	Δf
	0	250	500	0	250	500	0	250	500	0	250	500
-35	621/7	436	431	768/35	453	436	835/47	468	454	827/48	484	500
-40	541	461	-	806/34	432	443	826/46	460	460	826/49	468	486
-45	566/2	-	-	806/36	-	441	820/42	442	454	830/51	440	442
-50	594/2	-	-	758/29	-	-	811/46	465	-	833/47	450	456

(b). Two strong signals case

SNR	T = 10			T = 50			T = 100			T = 150		
	Δf	Δf	Δf	Δf	Δf	Δf	Δf	Δf	Δf	Δf	Δf	Δf
	0	250	500	0	250	500	0	250	500	0	250	500
-35	767/12	462	460	808/50	455	462	894/59	468	454	873/62	454	470
-40	676/13	-	447	840/48	469	441	882/61	460	460	864/63	460	462
-45	685/10	-	-	814/46	443	-	892/59	442	454	871/64	440	442
-50	750/19	-	-	889/45	408	-	905/58	-	-	881/62	423	463

(c). Three strong signals case

SNR	T = 10			T = 50			T = 100			T = 150		
	Δf	Δf	Δf	Δf	Δf	Δf	Δf	Δf	Δf	Δf	Δf	Δf
	0	250	500	0	250	500	0	250	500	0	250	500
-35	789/10	425	429	973/62	441	447	887/62	468	454	887/65	464	460
-40	897/22	-	437	887/65	438	439	876/64	448	464	870/64	464	448
-45	875/30	-	-	853/66	-	-	872/66	438	434	890/64	450	440
-50	872/29	-	-	929/61	-	-	909/56	-	-	901/66	446	455

(d). Four strong signals case

Table 4. Number of acquisition searches in the presence of strong signals (- indicates not acquired)

5. CONCLUSIONS

Weak signal acquisition is a particular concern for GPS based indoor services like Wireless E911 etc. The cross correlation of local replica of the desired weak signal with a strong received GPS signal may exceed the detection threshold causing the false acquisition. This becomes worse as the number of interferers (strong received GPS signals) increases. This paper presents a detailed analysis of the L1-C/A cross correlation in the presence of multiple strong signals under different conditions of relative Doppler offsets and dwell times. Acquisition of weak signals (of different SNR levels) is performed under these conditions and the results are presented. The results identified that for relative Doppler offsets (relatively) away from d k Hz. ($d = 0, \pm 1, \pm 2, \ldots..$), extended dwell times significantly reduce the effect of cross correlation, leading to improved probability of detection.

ACKNOWLEDGEMENTS

This research work is supported by the Australian Research Council Discovery Project DP0556848.

REFERENCES

Dempster, A.G. (2006), Correlators for L2C: Some Considerations, Inside GNSS, pp32-37

Glennon E P and A G Dempster (2004), "A Review of GPS Cross Correlation Mitigation Techniques", Proc GNSS2004, Sydney, 6-8 Dec 2004

Glennon Éamonn P. and Andrew G. Dempster (2005), "A Novel GPS Cross Correlation Mitigation Technique", ION GNSS 18th International Technical Meeting of the Satellite Division, 13-16 September 2005, Long Beach, CA, pp. 190-199, 2005.

Kaplan, E D, and C J Hegarty, "Understanding GPS: Principles and Applications", 2nd ed., Artech House, 2006

Morton Jade, James B. Y. Tsui, David M. Lin, Liyeh. L. Liou, Mikel M. Miller, Qihou Zhou, Marcus P. French, John Schamus (2003), Assessment and Handling of CA Code Self-Interference during Weak GPS Signal Acquisition, ION GPS/GNSS, Portland OR.

Spilker J, Parkinson, James J. (1996) GPS Signal Structure and Theoretical Performance, Global Positioning System, Theory and Applications Vol. 1, Edited by B.W.

Shanmugam Surendran K.(2006), Improving GPS L1 C/A Code Correlation Properties Using a Novel Multi-correlator Differential Detection Technique, ION GNSS 2006, Fort Worth TX.

Tong, P. S. (1973), A Suboptimum Synchronization Procedure for Pseudo Noise Communication Systems, Proc. of National Telecommunications Conference, 1973, pp. 26D 1–26D-5.

Ward Phillip W., Betz J W., Hegarty C. J, Satellite Signal Acquisition, Tracking, and Data Demodulation, Chapter 5, Understanding GPS: Principles and Applications", 2nd ed., Artech House, 2006

Zarlink Semiconductor
http://assets.zarlink.com/DS/zarlink_GP2015_MAY_05.pdf